



ELSEVIER

Applied Catalysis A: General 181 (1999) 39–49



Post-synthetic preparations of titanium-containing mesopore molecular sieves

W.S. Ahn^{a,*}, D.H. Lee^a, T.J. Kim^b, J.H. Kim^b, G. Seo^b, R. Ryoo^c

^aDepartment of Chemical Engineering, Inha University, Incheon 402-751, South Korea

^bDepartment of Chemical Technology, Chonnam National University, Kwang Ju 500-757, South Korea

^cDepartment of Chemistry and Center for Molecular Science, KAIST, Taejon 305-751, South Korea

Received 19 June 1998; received in revised form 9 November 1998; accepted 13 November 1998

Abstract

Titanium-substituted mesoporous molecular sieves were prepared post-synthetically by applying Ti-butoxide in ethanol solutions of different concentrations to MCM-41, MCM-48, and KIT-1. The catalysts obtained were characterized by XRD, FT-IR, UV-Vis spectroscopies, XAS, and N₂ physisorption. Incorporation of Ti seems to promote further crosslinking of the mesoporous walls of the samples, and resulted in wall thickness increases. The post-synthetically prepared Ti-mesoporous derivatives using titanium butoxide grafting were catalytically active for the selective oxidation of 2,6-di-*tert*-butylphenol with H₂O₂. Their activities depended on the Ti concentration of the catalysts. Comparison works with hydrothermally prepared Ti-MCM-41, Ti-HMS or post-synthetically prepared Ti-mesopore catalysts, either using titanocene grafting or by TiCl₄ atom planting method, are also reported. © 1999 Elsevier Science B.V. All rights reserved.

Keywords: Titanium; Mesoporous molecular sieves; Peroxide oxidation; Post-synthesis

1. Introduction

Recently, synthesis and characterization of different types of mesoporous silicates such as MCM-41 [1–3], HMS [4], and MCM-48 [1,2] have been reported. They consist of a regular array of uniform one- or three-dimensional pores with diameters varying between 15 and 100 Å. In addition, a mesoporous material designated as KIT-1 with the channel arrangement interconnected in a three-dimensional disordered arrangement was prepared by adding various organic polyacids to the MCM-41 synthesis

ingredients [5]. By incorporating various redox metal species (Ti, V, Mn, Sn) isomorphously into these structures, we found that redox molecular sieves effective in large organic molecule transformations in liquid phase reactions had emerged. Usually such Ti-mesoporous redox molecular sieves were prepared by introducing a suitable titanium precursor during hydrothermal synthesis steps which proceed via surfactant templating mechanism of S⁺I⁻/S⁺X⁻I⁺, or S⁰I⁰ nature [6–8]. However, they can also be prepared more easily using various post-synthesis treatments, for example using titanocene [9], and there exists some scope to extend the previously known TS-1 synthesis methods such as atom planting technique using TiCl₄ vapor [10] to the post-synthetic prepara-

*Corresponding author. Tel.: +82-32-860-7466; fax: +82-32-872-0959; e-mail: whasahn@dragon.inha.ac.kr

tion of mesoporous redox molecular sieves. It is believed that pore walls of mesoporous silicates which do not possess an ordered structure, not like their microporous silicates counterparts, can offer diverse ways to incorporate redox metals by various post-synthetic treatments. In this study, we have proposed an alternative post-synthetic procedure to prepare a Ti-mesoporous silicate. Supporting characterization work as well as catalytic studies of 2,6-DTBP oxidation was conducted to demonstrate its physico-chemical properties as a redox molecular sieve.

2. Experimental

2.1. Synthesis

The post-synthetic procedure proposed by us for preparing Ti-containing mesoporous materials from pure silica analogs can be classified as a grafting technique. A calcined mesoporous material (MCM-41/MCM-48/KIT-1) was washed at 40°C for 2 h with dry ethanol solution. Subsequently, it was suspended in dry ethanol solution containing a calculated amount of titanium(IV) butoxide (TBOT, Aldrich, 99% solution) for 1 h with stirring. To eliminate excess TBOT, the filtered material was washed with dry ethanol solution three times, centrifuged, dried at 50°C and calcined in air at 550°C for 4 h. A series of titanium-substituted mesoporous molecular sieves were also prepared for comparison purposes. For hydrothermal synthesis of Ti-MCM-41, a procedure reported by Franke et al. [3] was used. A calculated amount of Ludox AS-40 (Du Pont, 40 wt% colloidal silica in water) were put into a polypropylene beaker and stirred with vigorous agitation. Tetraethyl ammonium hydroxide solution (TEAOH, Aldrich, 20 wt% solution in water) and subsequently 1/3 of the required cetyltrimethylammonium bromide (CTMABr, Aldrich) solution was added. To the gel formed, the rest of the surfactant and an appropriate amount of TBOT diluted with 2-propanol were added simultaneously. The gel was agitated for 30 min and then reacted statically in a 250 ml polypropylene autoclave at 105°C for 24 h. The reaction mixture of the sample corresponded to an oxide molar ratio of $\text{SiO}_2 : 0.02\text{-TiO}_2 : 0.2(\text{TEAOH}) : 0.25(\text{CTMABr}) : 31\text{H}_2\text{O}$. The resulting solid product was recovered by filtration,

extracted with ethanol for 4 h, washed several times with distilled water, and finally organic molecules which remained were removed by calcination in air at 540°C for 6 h.

For Ti-HMS, a hydrothermal procedure reported by Gontier and Tuel [4] was adopted. A solution was prepared by mixing TEOS (Aldrich, 98% solution) and TBOT dissolved in dry ethanol. The first solution was added slowly to the second solution that contains dodecylamine (DDA, Aldrich, 98%) and water under vigorous stirring. Stirring was maintained for about 15 min, and the solution was kept at ambient temperature for various periods with vigorous stirring. All vessels, except that with TBOT, were washed with 5.5 g of deionized water to achieve a quantitative transfer of reagents. As the vessel with TBOT could not be washed with water because of the hydrolysis, extra 0.05 g of TBOT were always added to make up for the losses. The rest of the procedure is identical to Ti-MCM-41. The reaction mixture of the samples corresponded to an oxide molar ratio of $\text{SiO}_2 : 0.02\text{-TiO}_2 : 0.2(\text{DDA}) : 9.0(\text{EtOH}) : 160\text{H}_2\text{O}$.

Grafted Ti-KIT-1 was prepared using titanocene by the procedure of Maschmeyer et al. [9]. Titanocene dichloride was dissolved in chloroform and allowed to penetrate into KIT-1 dry powder for 30 min. The treated KIT-1 was exposed in situ to triethylamine to activate the surface silanols of the KIT-1. The color of the suspension changed from red via orange to yellow, signifying the substitution of the chloride with alkoxide/siloxide ligands. After extensive washing with chloroform, organic components of this material were removed by calcination at 540°C under dry oxygen, leaving the white mesoporous catalysts (Si/Ti=20) powder.

Finally, Ti-KIT-1 was also prepared using TiCl_4 by an atom planting procedure. The TiCl_4 vapor (30 cm³/min) was allowed to contact pure dehydrated silicate KIT-1 at 500°C for 2 h, and then was cooled to room temperature, washed by deionized water, and dried at 80°C for 24 h.

Diverse synthesis methods have been used to prepare mesoporous titanium molecular sieves; in this work these will be denoted, respectively, by Ti-[material type](preparation method, Ti-source, Ti-contents). For the preparation methods, H stands for the usual hydrothermal procedure, G for grafting, and A for atomic planting. For the titanium source, TC repre-

sents titanocene, TB titanium butoxide, and TCL titanium chloride. Ti-MCM-41(G,TB,0.02), for example, is a sample of Ti-MCM-41 prepared according to grafting procedure using titanium butoxide to the pure silica form MCM-41 to 2 mol% Ti/(Ti+Si).

2.2. Characterization

The powder X-ray diffraction (XRD) patterns of all samples were measured on a Phillips PW3123 diffractometer equipped with a graphite monochromator and Cu K α radiation ($\lambda=1.5406 \text{ \AA}$). In general, the diffraction data were collected by using a continuous scan mode with a scan speed of one degree (2θ)/min.

Framework FT-IR spectra of samples were recorded in air at room temperature on a Perkin Elmer 221 spectrometer (in the range of 400–4000 cm^{-1}) with wafers of molecular sieves mixed with dry KBr. Two hundred scans were accumulated for each spectrum in transmission mode, at a spectral resolution of 4 cm^{-1} . The spectrum of dry KBr was also taken for background subtraction. UV-Vis spectroscopic measurements were carried out on a Varian CARY 3E double beam spectrometer connected with a computer and dehydrated MgO as a reference in the range of 190–820 nm. The X-ray absorption spectroscopy measurement was carried out above the Ti K edge (4966 eV) at room temperature using Beam Line 12C at the Photon Factory in Tsukuba, Japan. The injection beam energy was 2.5 GeV, and the monochromator was a Si(1 1 1) double crystal with a typical resolution of $\Delta E/E=1.1 \times 10^{-4}$ at the Ti K edge.

The nitrogen adsorption isotherms and specific surface areas were determined by nitrogen physisorption with the BET method at liquid nitrogen temperature using a Micromeritics ASAP 2000 automatic analyzer. Prior to measurement, the samples were degassed at 623 K for 6 h. The final pressure was ca. 0.1 Pa in the closed system for at least 1 min. BET surface areas were calculated in a relative pressure range between 0.01 and 0.1 assuming a cross-sectional area of 0.162 nm^2 for the nitrogen molecule.

2.3. Catalytic oxidation of organic compound

The catalytic activities of all samples were tested for the liquid phase oxidation of 2,6-di-*tert*-butylphenol (2,6-DTBP) to quinone using H $_2$ O $_2$ as an oxidant.

Reactions were performed under vigorous stirring in a two-neck glass flask equipped with a condenser and thermometer. The oxidation of 2,6-DTBP was carried out using 10 mmol of substrate, 100 mg of catalyst, 10 g of acetone as a solvent, and 30 mmol of 35 wt% H $_2$ O $_2$. The reaction was carried out at 333 K for 2 h, and the products were analyzed using a HP 5890 series II GC equipped with a HP-5 capillary column and an FID. The internal standard method was used for quantitative analysis of the products, and the conversions of substrate and selectivity to the products were calculated through carbon balance.

3. Results and discussion

Table 1 summarizes the structural properties of the Ti-substituted mesoporous molecular sieves prepared by hydrothermal and by post-synthetic procedures. The surface areas of all samples prepared ranged from ca. 750 to ca. 1350 m^2/g , being typical of M41S group materials. As for the hydrothermally synthesized Ti-MCM-41 and Ti-HMS, no clear influence of Ti content on the unit cell parameter was observed, as reported by Blasco et al. [11]. However, BJH pore diameter of these samples decreased upon Ti introduction, and consequently the corresponding measure of wall thickness estimated by the difference between the unit cell parameter and BJH pore diameter showed increases upon Ti-introduction. These increases in framework wall thickness indicate Ti incorporation in the walls of the mesoporous silicate framework [3,11]. Generally, much the same trend is observed with increases in Ti-contents. For the post-synthetically prepared Ti-mesopore samples using titanium butoxide, titanocene, or TiCl $_4$, unit cell size and wall thickness increased relative to those of the pure silica mesopore materials.

Fig. 1 shows the various XRD patterns of calcined Ti-mesoporous materials, together with corresponding pure silica analogs. Both MCM-41 and KIT-1 samples exhibit well-defined (1 0 0) reflections in their XRD patterns. These (1 0 0) reflections moved slightly to the left and concurrently long range order of MCM-41 diminished somewhat as Ti is incorporated. For MCM-48, (2 1 1) and (2 2 0) reflections are clearly visible and other long range order minor peaks are also well resolved; much the same feature was retained

Table 1
Structural data of Ti-mesoporous materials

Sample ^a	<i>d</i> -Value	Unit cell (Å) ^b	BET surface area (m ² /g)	BJH average pore diameter (Å)
MCM-41	38.9	44.9	966	38.0
Ti-MCM-41(H,0.02)	40.7	47.0	1135	31.7
Ti-MCM-41(H,0.038)	40.0	46.2	1068	28.3
HMS	39.2	45.3	962	36.3
Ti-HMS(H,0.02) ^c	34.4	39.7	1265	25.9
Ti-HMS(H,0.02) ^d	35.2	40.6	1363	25.0
MCM-48	36.2 (<i>d</i> _{2 1 1})	88.7	1272	29.9
Ti-MCM-48(G,TB,0.02)	36.6 (<i>d</i> _{2 1 1})	89.7	963	30.9
KIT-1	41.7	48.2	948	33.9
Ti-KIT-1(G,TB,0.014)	44.7	51.6	925	32.9
Ti-KIT-1(G,TB,0.063)	43.0	49.6	989	32.8
Ti-KIT-1(G,TB,0.121)	43.6	50.3	869	31.3
Ti-KIT-1(G,TC,0.048)	45.7	52.8	947	32.8
Ti-KIT-1(G,TC,0.09)	44.5	51.4	749	29.5
Ti-KIT-1(A,TCL,-) ^e	45.2	52.1	907	32.7

^aFor Ti-mesoporous materials prepared by titanium butoxide grafting, Ti-contents of the sample were measured by EDX. Other figures correspond to the TiO₂/SiO₂ content of the mother liquid.

^bThe unit cell parameter is $2d_{100}/\sqrt{3}$ for hexagonal structure and $d_{211} \times \sqrt{(h^2 + k^2 + l^2)}$ for cubic structure.

^cCrystallization time 8 h.

^d20 h.

^eTiCl₄, 30 cm³/min for 2 h.

even after Ti incorporation by titanium butoxide grafting. These XRD patterns confirm that structural integrity of the mesoporous materials remained intact after post-synthetic treatment.

Fig. 2 presents the N₂ adsorption isotherms and the corresponding BJH pore size distribution curves for Ti-KIT-1 samples prepared by titanium butoxide grafting. The abrupt increases in the $P/P_0=0.2-0.35$ region and the corresponding maxima in the pore size distribution curves indicate the uniform mesopores of ca. 3.2 nm diameter. The BJH data showed approximately 20 Å distribution from the mean pore diameter for pure silica KIT-1, and this matches well with other distribution curves reported earlier [12,13]. Since titanium species introduced post-synthetically would be expected to react with surface silanol groups of the walls in a random fashion, the pores with largest population would make a contact with titanium species in relatively high probability. As a consequence, as the amount of grafted titanium species increases, slight reduction in average pore size was observed, accompanied by broadness in distribution around the average pore diameters.

The FT-IR spectra of the titanium grafted and hydrothermally prepared Ti-mesoporous molecular sieves are given in Fig. 3. A band at 960 cm⁻¹ is clearly visible in all spectra. For Ti-containing zeolites, the band at 960 cm⁻¹ is believed to be a consequence of stretching vibrations of SiO₄ tetrahedra bound to the Ti atoms, that is, Si–O–Ti bonds and its systematic increase in intensity with the Ti content is generally taken as a proof of the incorporation of titanium into the framework [14]. However, the 960 cm⁻¹ band also occurs in the spectra of Ti-free mesoporous molecular sieves due to the abundance of silanol groups present in the calcined samples and cannot be used as a criterion to claim the incorporation of titanium into the framework [11].

UV–Vis DRS spectra of the calcined Ti-mesoporous materials are given in Fig. 4. The spectra of Ti-containing mesoporous materials were characterized by broader absorption bands centered at 220 and 260–270 nm, as reported by Zhang et al. [6,7]. For TS-1 [15] and Ti-Beta [16], an intense band at ca. 220 nm has been assigned to the ligand-to-metal charge transfer involving isolated Ti atoms in octahedral coordi-

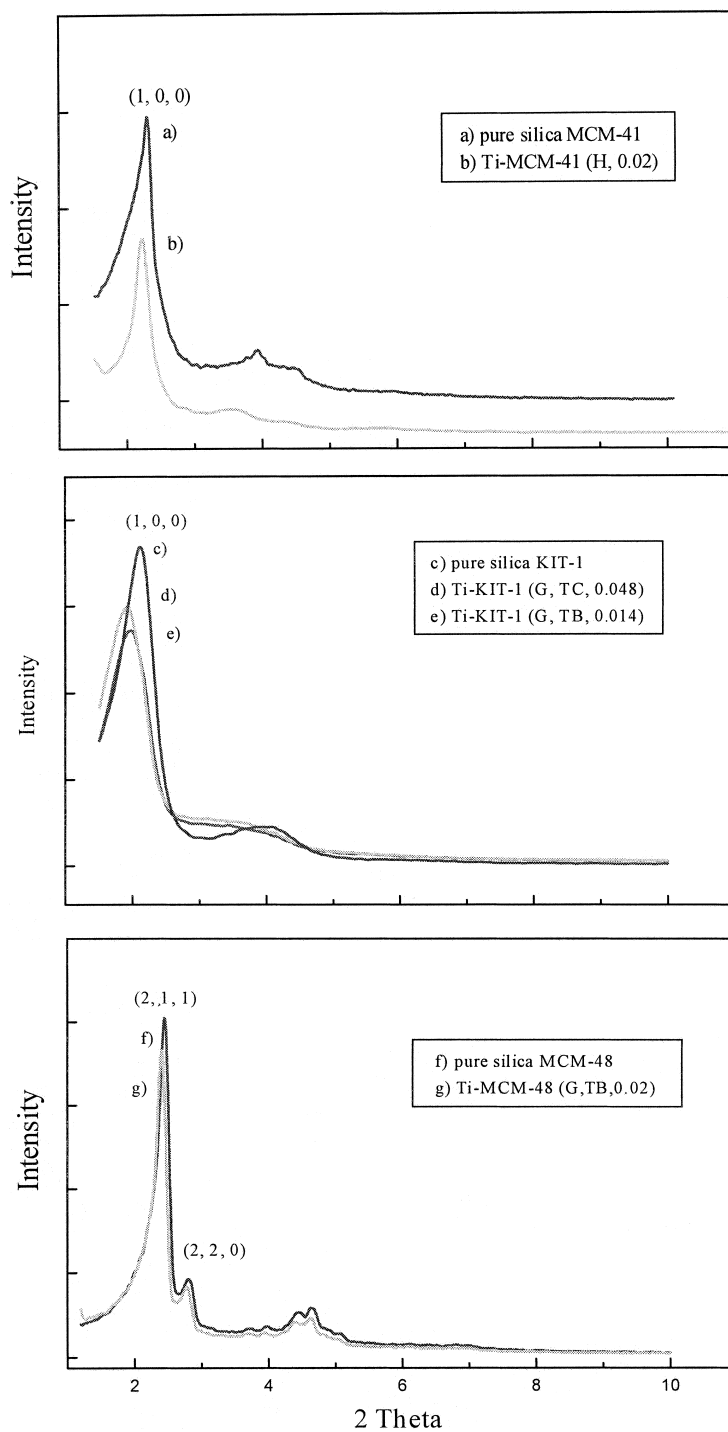
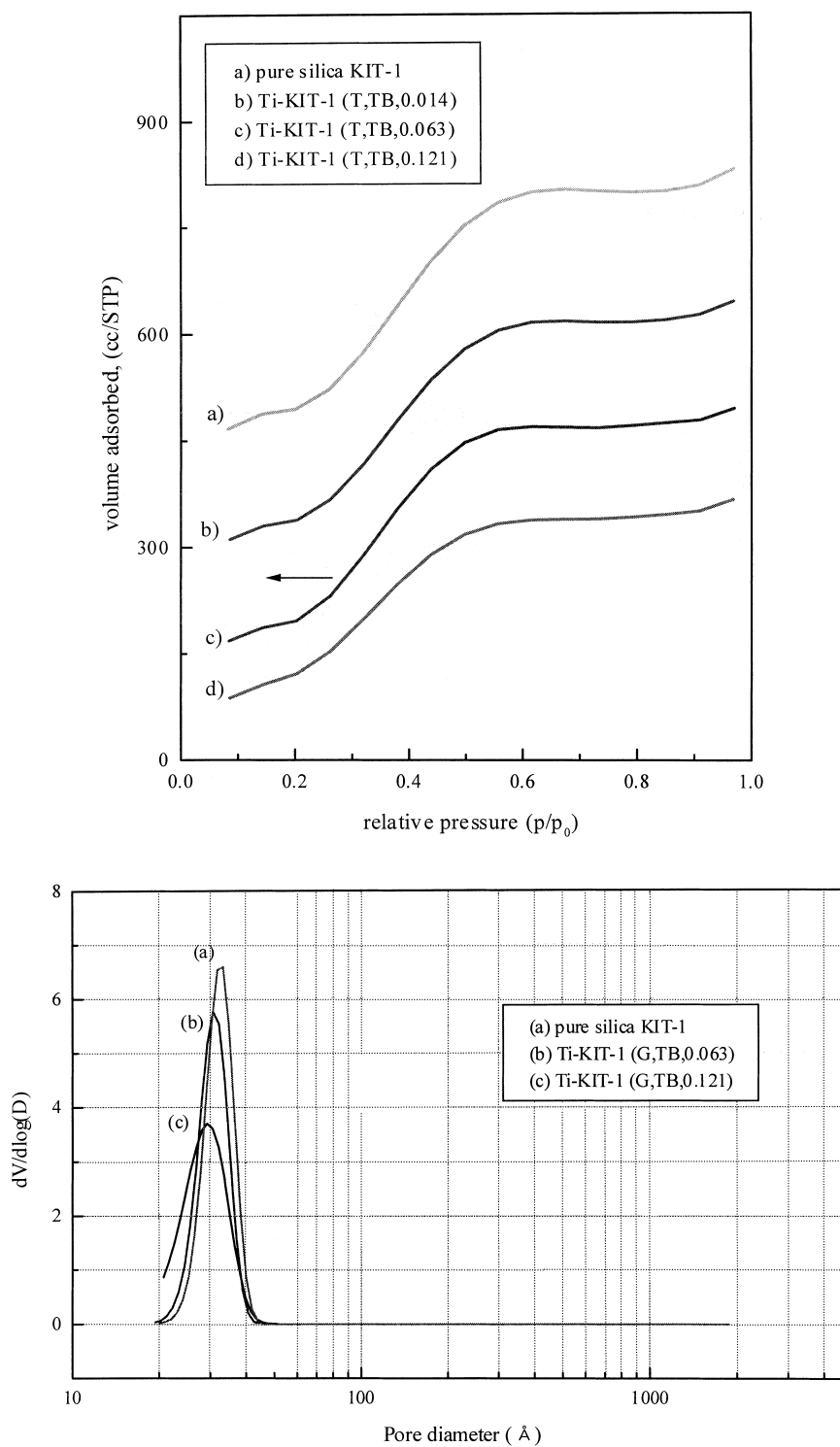


Fig. 1. XRD spectra of Ti-substituted mesoporous molecular sieves.

Fig. 2. Adsorption isotherm and $dV/d\log(D)$ vs. pore diameter plot of Ti-substituted mesoporous molecular sieves.

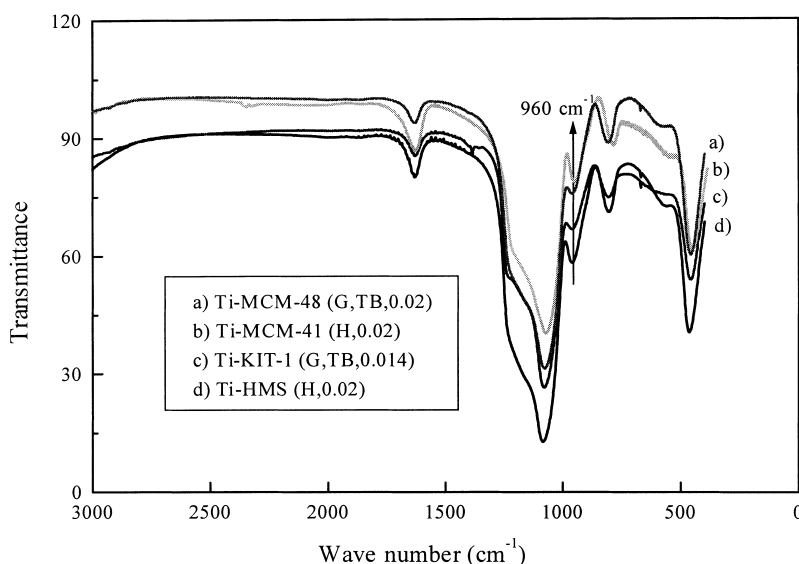


Fig. 3. FT-IR spectra of Ti-substituted mesoporous molecular sieves.

nation, in which two water molecules form part of the metal coordination sphere. According to this assignment, the band at ca. 220 nm in Ti-substituted mesoporous materials may be associated with isolated Ti(IV) framework sites fundamentally similar in character to those in TS-1. The shoulder at 270 nm probably corresponds to partially polymerized hexacoordinated Ti species [15], and some Ti–O–Ti clusters are suspected to co-exist with the isolated Ti sites in all the mesoporous samples prepared. A broad absorption band occurring at 325 nm is typical for ligand-to-metal charge transfer in bulk titania. Absence of a shoulder at \sim 330 nm indicates that Ti-containing MCM-41, MCM-48, and KIT-1 samples prepared by both hydrothermal (b)(d) or grafting methods (c)(k)(o)(p) are free of anatase phase. Ti-KIT-1 sample prepared by atom planting using TiCl_4 (g), on the other hand, is more susceptible to anatase formation and shows a distinctive shoulder at 330 nm. The band centered at ca. 220 nm in UV–Vis DRS spectra grew in intensity as the amount of titanium incorporated by post-synthetic treatment with titanium butoxide increased, as in KIT-1(k)(j)(i) or in MCM-41(p)(o)(n)(m). Partially polymerized hexacoordinated Ti species also grows concurrently in Ti-containing MCM-41 and KIT-1 samples; above ca. 6% of titanium, its population seems to have reached a significant but steady level. No anatase

phase was, however, detected in XRD, even for sample (m).

XANES spectrum of the calcined Ti-mesoporous material, Ti-KIT-1(G,TB,0.121) is given in Fig. 5. A single strong pre-edge peak which can be assigned as titanium species in tetrahedral or distorted octahedral symmetry due to hydration [11] is clearly visible for this sample, and this feature is quite different from the multiple low-intensity pre-edge peaks of anatase or rutile. Ti-grafted samples with lower titanium contents are also expected to be free from the bulk phase titania. The qualitative information deduced from the XANES has been complemented by the EXAFS analysis. We have taken the EXAFS data using a sample exposed to air in a transmission mode. EXAFS data were analyzed using the UWXAFS 2 program package [17], and Ti–O coordination number and its inter-atomic distance were estimated to be 5.1 and 0.190 nm, respectively. These values are slightly higher than 4 and 0.181 nm reported by Maschmeyer et al. [9] for titanocene-grafted MCM-41 samples. The higher coordination Ti-sites are most likely generated through hydration of the tetrahedrally coordinated sites [6,7,18]. Further work on the EXAFS analysis is in progress.

The catalytic activity of hydrothermally prepared Ti-MCM-41 or Ti-HMS for the epoxidation of 1-hexene and norbornene [19] or oxidation of aromatic

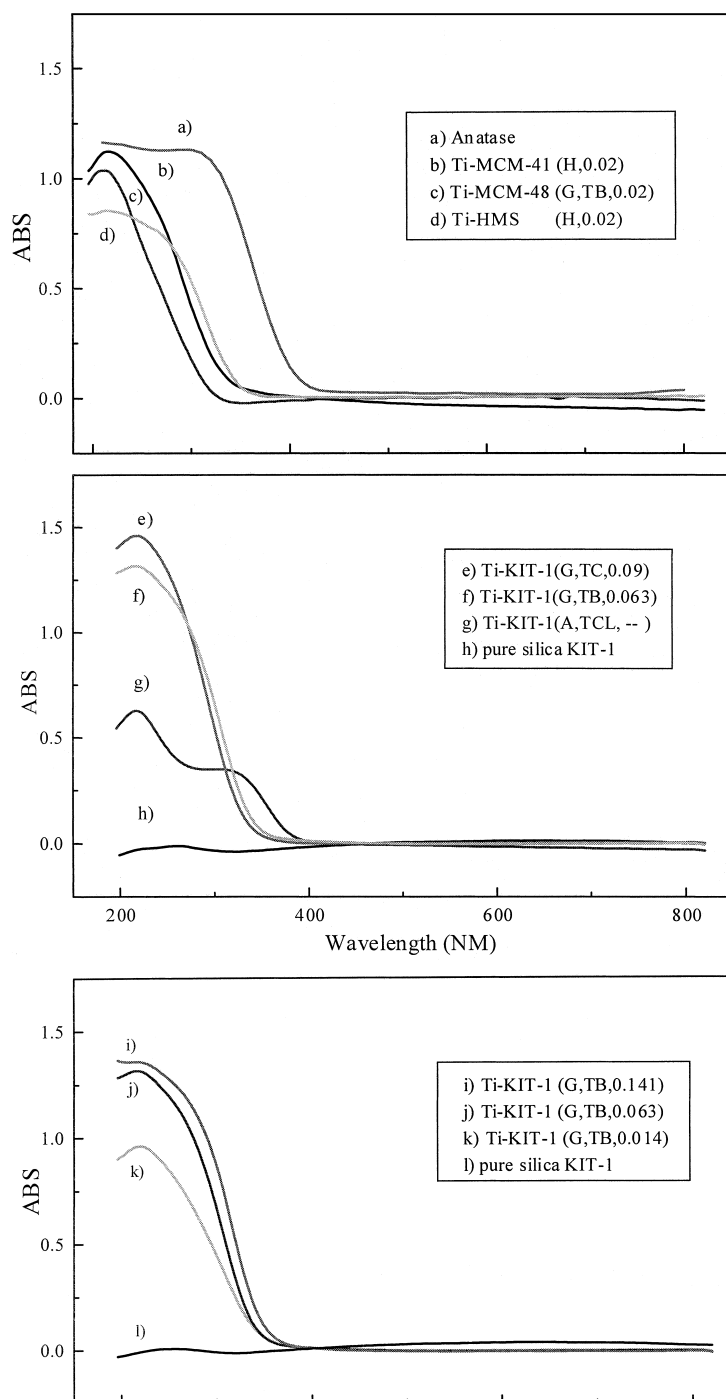


Fig. 4. UV-Vis spectra of Ti-mesoporous molecular sieves.

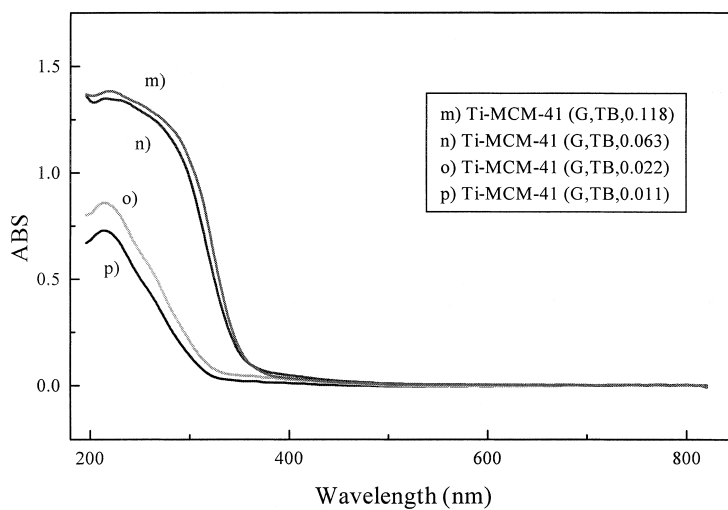


Fig. 4. (Continued)

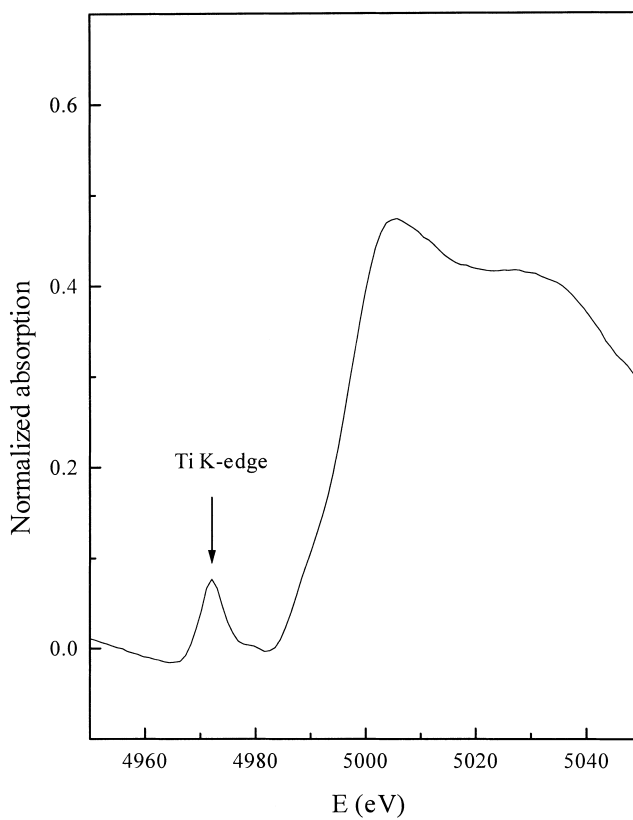


Fig. 5. XANES spectrum of Ti-KIT-1(G,TB, 0.121).

Table 2
Catalytic reactions of Ti-substituted mesoporous materials

Catalysts	2,6-DTBP conversion (mol%)	H ₂ O ₂ ^a conversion (mol%)	H ₂ O ₂ ^b selectivity (mol%)
Pure silica KIT-1	<5		
Ti-MCM-41(H,0.02)	15	24	42
Ti-HMS(H,0.02)	22	29	51
Ti-MCM-48(G,TB,0.02)	18	20	60
Ti-KIT-1(G,TB,0.014)	22	29	51
Ti-KIT-1(G,TB,0.063)	31	39	53
Ti-KIT-1(G,TB,0.121)	38	42	60
Ti-KIT-1(G,TB,0.121) ^c	33	35	63
Ti-KIT-1(G,TB,0.121) ^d	35	42	56
Ti-KIT-1(G,TB,0.141) ^e	32	63	34
Ti-KIT-1(G,TC,0.048)	24	31	52
Ti-KIT-1(G,TC,0.09)	26	34	51
Ti-KIT-1(A,TCL,-)	14	19	49
Ti-MCM-41(G,TB,0.011)	13	20	43
Ti-MCM-41(G,TB,0.063)	28	37	50
Ti-MCM-41(G,TB,0.118)	32	45	47

^aH₂O₂ conversion was determined by titration with a 0.1 N KMnO₄ aqueous solution.

^bH₂O₂ selectivity was calculated based on the reaction stoichiometry of [2,6-DTBP]+2[H₂O₂] \rightarrow [Quinone]+3[H₂O].

^cAfter EtOH–HCl washing, 2 h.

^dWithout calcination.

^eWithout EtOH washing.

^fQuinone selectivities were greater than ca. 98% for all runs.

substrates of different size [6,7] was reported. These studies have demonstrated that Ti-MCM-41 and Ti-HMS are effective oxidation catalysts for bulky aromatic components that cannot be converted over the microporous TS-1. In this work, catalytic performance of the various Ti-containing mesoporous materials for the oxidation of relatively bulky aromatic compound, 2,6-DTBP was conducted. The catalytic results are summarized in Table 2. As for the oxidation of 2,6-DTBP, Ti-KIT-1 post-synthetically prepared using high concentration of titanium butoxide showed the best performance. The order of catalyst activity was observed as Ti-KIT-1(G,TB,0.121)>Ti-MCM-41(G,TB,0.118)>Ti-KIT-1(G,TC,0.09)>Ti-HMS(H,0.02)>Ti-MCM-41(H,0.02)>Ti-KIT-1(A,TCL,-). For approximately the same concentration of titanium contents of 2 mol%, Ti-HMS performed better than Ti-MCM-41 as reported [6,7], and Ti-MCM-48 or Ti-KIT-1 was also better than Ti-MCM-41, due possibly to the three-dimensional pore structure of the former [20]. The catalytic activities of titanocene-grafted samples were almost identical whether 4.8 or 9 mol% titanium loading was attempted. It seems that chloroform washing after grafting leaves the KIT-1

with virtually the same concentration of titanium within the mesopore structure. Among the titanium butoxide-grafted MCM-41 or KIT-1 samples, 2,6-DTBP conversion increased as the titanium contents increased. For Ti-KIT-1(G,TB,0.121), acid washing to remove the possible extra-framework Ti species resulted in a decrease in conversion, accompanied by a slight increase in H₂O₂ selectivity, implying that isolated titanium as well as extra-framework Ti species may be removed, as was the case in TS-1 [21]. Bulk titania or substituted silicas containing Ti–O–Ti bonds present in zeolites are not suitable for catalytic peroxide oxidation reaction because they selectively decompose H₂O₂ [22].

Calcination proved to have little effect on the catalytic performance, but ethanol washing after titanium butoxide grafting seems essential to achieve the high H₂O₂ selectivity; EDX showed that extra-framework Ti species may further accumulate in the grafted Ti-KIT-1 without ethanol washing. In order to verify the chemical stability of the titanium butoxide-grafted samples, a reaction was run using the catalyst Ti-KIT-1(G,TB,0.121) for 2 h and subsequently the catalyst was hot filtered and the filtrate was allowed to react

further at the same reaction temperature. Virtually the same conversion was obtained even after the filtrate reaction, and the grafted sample did not show any evidence of metal leaching.

4. Conclusions

In summary, the following conclusions have been emerged from the above experiments:

1. Titanium-substituted derivatives of the mesoporous molecular sieves (MCM-41, MCM-48, HMS and KIT-1) can be prepared by post-synthetic methods using Ti-butoxide or titanocene grafting without destroying the mesopore structure.
2. Incorporation of Ti either by hydrothermal or by post-synthetic treatments likely promotes the further crosslinking of the pore walls of all mesoporous materials, and both resulted in wall thickness enhancement upon Ti-introduction.
3. Titanium introduced by Ti-butoxide grafting method is mostly located in the structural framework in Ti-mesoporous molecular sieves, but some polymeric titanium species may coexist, and such extra-framework species steadily increases with the amount of titanium used in the treatment.
4. Ti-substituted mesoporous derivatives both prepared by hydrothermal and post-synthetic method were catalytically active for the selective oxidation of 2,6-DTBP with H_2O_2 . Pronounced catalytic activity enhancement was observed for Ti-KIT-1 prepared post-synthetically using Ti-butoxide, due to the high titanium contents introduced.

Acknowledgements

This work has been supported by the fund provided by KOSEF through research grant no. 97-05-02-06-01-3.

References

- [1] C.T. Kresge, M.E. Leonowicz, W.J. Roth, J.C. Vartuli, J.S. Beck, *Nature* 359 (1992) 710.
- [2] J.S. Beck, J.C. Vartuli, W.J. Roth, M.E. Leonowicz, C.T. Kresge, K.D. Schmitt, C.T.-W. Chu, D.H. Olson, E.W. Sheppard, S.B. McCullen, J.B. Higgins, J.L. Schlenker, *J. Am. Chem. Soc.* 114 (1992) 10834.
- [3] O. Franke, J. Rathousky, G. Schulz-Ekloff, J. Starek, A. Zukal, *Stud. Surf. Sci. Catal.* 84 (1994) 77.
- [4] S. Gontier, A. Tuel, *Zeolites* 15 (1995) 601.
- [5] R. Ryoo, J.M. Kim, C.H. Shin, J.Y. Lee, *Stud. Surf. Sci. Catal.* 105 (1997) 45.
- [6] W. Zhang, J. Wang, P.T. Tanev, T.J. Pinnavaia, *J. Chem. Soc., Chem. Commun.* (1996) 976.
- [7] W. Zhang, M. Froba, J. Wang, P.T. Tanev, J. Wong, T.J. Pinnavaia, *J. Am. Chem. Soc.* 118 (1996) 9164.
- [8] K.A. Koyano, T. Tatsumi, *Microporous Mater.* 10 (1997) 259.
- [9] T. Maschmeyer, F. Rey, G. Sankar, J.M. Thomas, *Nature* 378 (1995) 159.
- [10] P. Wu, T. Komatsu, T. Yashima, *J. Phys. Chem.* 100 (1996) 10316.
- [11] T. Blasco, A. Corma, M.T. Navarro, J.P. Pariente, *J. Catal.* 156 (1994) 65.
- [12] Z. Luan, H. He, W. Zhou, C. Cheng, J. Klinowski, *J. Chem. Soc., Faraday Trans.* 91(17) (1995) 2955.
- [13] V.V. Gusev, X. Feng, Z. Bu, G.L. Haller, J.A. O'Brien, *J. Phys. Chem.* 100(6) (1996) 1985.
- [14] M.R. Boccuti, K.M. Rao, A. Zecchina, G. Leofanti, G. Petrini, *Stud. Surf. Sci. Catal.* 48 (1989) 133.
- [15] G. Petrini, A. Cesana, G. De Alberti, F. Genoni, G. Leofanti, M. Padovan, G. Papparatto, P. Roffia, *Stud. Surf. Sci. Catal.* 68 (1991) 761.
- [16] T. Blasco, M.A. Cambor, A. Corma, J. Perez-Pariente, *J. Am. Chem. Soc.* 115 (1991) 11806.
- [17] A.I. Frenkel, E.A. Stern, M. Qian, M. Newville, *Phys. Rev. B* 48 (1993) 12449.
- [18] C.A. Yarker, P.A. Johnson, A.C. Wright, J. Wong, R.B. Gregor, F.W. Lytle, R.N. Sinclair, *J. Non-Cryst. Solids* 79 (1986) 117.
- [19] A. Corma, M.T. Navarro, J. Perez-Pariente, *J. Chem. Soc., Chem. Commun.* (1994) 147.
- [20] K.A. Koyano, T. Tatsumi, *J. Chem. Soc., Chem. Commun.* (1996) 145.
- [21] C.B. Khouw, M.E. Davis, *J. Catal.* 151 (1995) 77.
- [22] B. Nortari, *Stud. Surf. Sci. Catal.* 37 (1988) 413.